WILEY | Hindawi

Retraction

Retracted: Geological Mineral Energy and Classification Based on Machine Learning

Wireless Communications and Mobile Computing

This article has been retracted by Hindawi, as publisher, following an investigation undertaken by the publisher [1]. This investigation has uncovered evidence of systematic manipulation of the publication and peer-review process. We cannot, therefore, vouch for the reliability or integrity of this article.

Please note that this notice is intended solely to alert readers that the peer-review process of this article has been compromised.

Wiley and Hindawi regret that the usual quality checks did not identify these issues before publication and have since put additional measures in place to safeguard research integrity.

We wish to credit our Research Integrity and Research Publishing teams and anonymous and named external researchers and research integrity experts for contributing to this investigation.

The corresponding author, as the representative of all authors, has been given the opportunity to register their agreement or disagreement to this retraction. We have kept a record of any response received.

References

[1] Y. Lv and L. Lu, "Geological Mineral Energy and Classification Based on Machine Learning," *Wireless Communications and Mobile Computing*, vol. 2021, Article ID 2788161, 7 pages, 2021.

WILEY | Hindawi

Research Article

Geological Mineral Energy and Classification Based on Machine Learning

Yan Lv [ID] **and Laijun Lu** [ID]

College of Earth Sciences, Jilin University, Changchun Jinlin, 130061, China

Correspondence should be addressed to Yan Lv; 1530509005@stu.suda.edu.cn

In order to mine geological mineral energy and study on geological mineral energy classification, a method based on a wireless sensor was proposed. Of logistic regression, artificial neural networks, random forests, and main wireless sensor algorithms of support vector machine (SVM) with the model in the application of the energy mineral resource prediction practice effects are reviewed and discuss the practical application in the process of sample selection, the wrong points existing in the cost, the uncertainty evaluation, and performance evaluation of the model using wireless sensor algorithm, random forest of the probability distribution of mineralization in the study area is calculated, and five prospecting potential areas are delineated. The results show that the ratio of ore-bearing unit and non-ore-bearing unit is 1 : 1, and the best random forest training model is obtained. 70% of the training sample set was randomly selected as the training set, and the remaining 30% was used as the test set to construct the random forest model. The training accuracy of the model is 96.7%, and the testing accuracy is 96.5%. Both model training accuracy and model testing accuracy are very high, which proves the accuracy of RF model construction and achieves satisfactory results. In this study, a wireless sensor is successfully applied to 3D mineral energy prediction, which makes a positive exploration for mineral resource prediction and evaluation in the future. Finally, the prediction of mineral resource energy based on a wireless sensor is an important trend of future development.

1. Introduction

The reserves of mineral resources are a symbol of economic development. With the increasing social demand for mineral resources and the increasing difficulty of prospecting for mineral resources, the research on new theories and methods of prediction and evaluation of mineral resource energy has been promoted. Mineral resource energy evaluation has gone through three stages: the stage of mineral deposit statistical prediction, marked by the application of probability statistics and multivariate statistics [1]. The stage of resource and energy prediction and evaluation based on the theory of seeking difference is mainly marked by the theory and method of "geological anomaly mineralization and metallogenic prediction" initiated in 1990 and "comprehensive information metallogenic prediction" [2]. In the stage of "digital ore prospecting" and resource and energy prediction and evaluation, the application of data science in mineral

exploration is emphasized, and the practical problems in mineral exploration are solved by data analysis theory and method, with "triple" metallogenic prediction and resource evaluation theory and method as the main symbol [3]. The introduction of nonlinear and complexity theory and model into mineral resource evaluation is a rising research field in the world, and the representative one is the prediction theory and model of multiple formation proposed by Cheng Qiuming. In recent years, with the advent of the age of geological information, all kinds of geological data show an explosive growth trend, which brings challenges and opportunities to the development and innovation of mineral resource prediction and evaluation theories and methods. In order to solve the high dimension, high computational complexity, and uncertainty and realize multisource heterogeneous prospecting space data intelligent mining and integration, wireless sensor methods to dig deeper into the geological data, information fusion, and prediction

evaluation provide a useful tool and have become the focus in the current energy mineral resource prediction and frontier [4].

The core of mineral prediction is feature extraction and integration of geospatial data. The current research focus and frontier focus on feature extraction and integration of deep-level mineralized information. Deep mineralization information refers to the mineralization information that is difficult to be identified by traditional methods and technologies, including hidden mineralization information, deep mineralization information, and specific information extracted under complex geological background [5]. Mining and integration of deep mineralization information are the keys to successfully discover concealed ore and deep ore. In the era of big data, how to carry out deep-level mineralization information mining and integration based on a wireless sensor is the frontier field of mineral prediction [6]. Nurmaini et al. found in the study that when large sample MNIST data set was used, SVM accuracy was 0.88 and CNN accuracy was 0.98. When the small sample COREL1000 data set was used, the accuracy of SVM was 0.86 and CNN was 0.83 [7]. Aravinda and Lin proposed the 3D prediction process of deep mineral resources, namely, "geological information integration - quantitative extraction of metallogenic information - three-dimensional quantitative prediction," and studied the 3D quantitative analysis of geological body shape, quantitative extraction of ore-controlling geological factors, and three-dimensional quantitative prediction of ore bodies [8]. Siomos et al., with the application of three-dimensional comprehensive information metallogenic prediction method, carried out a case study on large-scale three-dimensional metallogenic prediction [9].

Based on this, this paper proposes a method based on a wireless sensor. Random forest has higher prediction accuracy and stability and can make energy evaluation on the importance of ore control elements. This study has successfully applied a wireless sensor to 3D mineral energy prediction, which makes a positive exploration for mineral resource prediction and evaluation in the future.

2. Mineral Resource Prediction by a Wireless Sensor

2.1. Random Forest Algorithm. Random forest is an important ensemble algorithm in the wireless sensor model. It is a combinatorial classifier composed of a decision tree classifier set proposed by Breiman in 2001 on the basis of decision tree and bagging method. The basic idea of random forest is to merge multiple unrelated decision trees together, and each tree has the same distribution [10, 11]. The classification error of the model depends on the classification ability of the decision tree and the correlation between the trees. For the classification algorithm, the new input samples are classified and predicted according to the decision tree in the forest.

2.1.1. Decision Tree. Decision tree is also a prediction model in a wireless sensor, which represents the mapping between object attributes and object values. It uses the structure of tree to divide data records into three types of nodes: root node, middle node, and leaf node. A leaf node of tree represents the record set corresponding to the leaf node of decision tree under certain conditions. The decision tree is generated by repeatedly establishing lower-level nodes in branch subsets [12]. CART is a typical binary decision tree, which can do both classification and regression. The CART algorithm uses the Gini coefficient as impurity to measure the impurity of a set sample. For a classification problem with characteristic variable M, there are n samples in the training sample set T; then, the Gini coefficient of the training sample set is

$$G(T) = 1 - \sum_{i=1}^{n} P_i^2. \tag{1}$$

In the formula, P_i represents the conditional probability of the occurrence of the ith category in the classification results. According to a certain classification standard S (such as j attribute values of attribute A), the sample is divided into K subsets, which are, respectively, $T_1, T_2, \cdots, T_k$; then, the Gini coefficient of this classification is

$$G(T, S) = \sum_{i=1}^{k} \frac{n_i}{n} * G(T_i). \tag{2}$$

The smaller the Gini coefficient is, the higher the purity of the subsample after dichotomy is, and the branching of the decision tree generated by this splitting method can represent the direct difference between different categories, because the division standard S with the minimum Gini coefficient is selected as the optimal splitting attribute and the optimal splitting node [13].

2.1.2. Bagging Method. The bagging method, also known as the self-help method, adopts equiprobabilistic random repeated sampling technique with put back to select training data to construct classifier and finally combine. In other words, every time a fixed number of samples are randomly collected from the original training set, the samples are put back and the next round of random sampling is conducted again. Since the data outside the bag does not participate in the model fitting, it can be used to estimate the classification accuracy without bias. The realization process is as follows: (1) T training samples are extracted from the original sample set D with the method of random sampling with replacement in each round, and n independent training sets are obtained through n rounds of extraction. (2) The NTH weak learner is obtained by using a training set Dn each time. (3) For the classification problem, the final strong learner can be obtained by adopting the majority voting method for the N weak learners obtained in the previous step; (4) for regression problems, the arithmetic mean of regression results is used as the final strong learner. Random forest is applied to mineral prediction, and its characteristic variables are the ore-controlling elements in the energy

prediction model, and its classification ability is used to judge the characteristics of ore-bearing attributes [14–16].

2.2. Support Vector Machine Regression Model

2.2.1. Model Principle. Support vector machine (SVM) is based on the statistical learning theory developed wireless sensor method, it can be through the kernel function can be used to convert the actual problem to high-dimensional feature space and through the structure in the high-dimensional space linear discriminant function to realize nonlinear discriminant in the original space, usually can get global optimal solution of support vector machine (SVM). Moreover, it has good generalization ability for large volume and high-dimensional data sets. In this chapter, the principle of the SVM model is firstly described based on the classification model, and then, it is extended to regression problems. The basic principles of the SVM model are as follows:

Let me define my matrix $m \times n$, X, and my column vector W, Y, where X is the input variable; x_i is the column vector: $[x_1, x_2, x_3, \cdots x_n]^T$; m is the sample number; n is the number of attribute features; W is the corresponding weight; and Y is the output variable.

$$
\begin{aligned}
X &= [x_1, x_2, x_3, \cdots x_m], \\
Y &= [y_1, y_2, y_3, \cdots y_m], \\
W &= [w_1, w_2, w_3, \cdots w_n].
\end{aligned}
\tag{3}
$$

The partition hyperplane in the sample space is defined by a linear equation:

$$
W^T X + b = 0.
\tag{4}
$$

In the formula, normal vector W determines the direction of the hyperplane. The displacement term b determines the distance between the hyperplane and the origin. In this definition, the distance between any point x in the sample space and the hyperplane is

$$
r = \frac{|W^T X + b|}{\|W\|}.
\tag{5}
$$

Considering the dichotomous problem, in order to obtain a good classification effect, if all samples are correctly classified, the sample points should meet the following constraints:

$$
y_i = \begin{cases} +1, & W^T x_i + b \geq +1, \\ -1, & W^T x_i + b \leq -1. \end{cases}
\tag{6}
$$

The training sample point closest to the hyperplane and satisfying formula (5) is defined as the support vector; then, the sum of the distance between the two dissimilar support

vectors and the hyperplane is defined as

$$
\gamma = \frac{2}{\|W\|}.
\tag{7}
$$

In the formula, γ is called interval, and the support vector machine algorithm is to find the hyperplane with the maximum interval γ, that is, to find the model parameter W, b that satisfies the constraint of formula (5) and maximizes γ:

$$
\max_{W,b} \frac{2}{\|W\|} \text{ s.t. } y_i(w^T x_i + b) \geq 1, \quad i = 1, 2, \cdots, m.
\tag{8}
$$

Obviously, in order to maximize the interval, only maximizing $\|W\|^{-1}$ is equivalent to minimizing $\|W\|^2$, and the relaxation factor ξ and regularization parameter C are added on this basis:

$$
\min_{w,b} \frac{1}{2}\|W\|^2 + C \sum_{i=1}^{m} \xi_i \text{ s.t. } y_i(w^T x_i + b) \geq 1 - \xi_i, \quad i = 1, 2, \cdots, m.
\tag{9}
$$

The duality problem can be obtained through the Lagrange bearing method used for (9):

$$
L(w, b, \xi, a, \mu) = \frac{1}{2}\|w\|^2 + C\sum\xi - \sum a\{y(w^T X + b) - 1 + \xi\} - \sum\mu\xi.
\tag{10}
$$

The support vector machine model with maximum soft interval can be obtained by solving the equation above, where the relaxation factor ξ is the classification error term. The degree of punishment for misclassification samples is controlled by regularization parameter C.

The SVM classification model is extended to the regression problem, and the error function with regularization term in the linear regression model is considered:

$$
\frac{1}{2}\sum_{n=1}^{N}\{h(x_n, w) - y_n\}^2 + \frac{\lambda}{2}\|w\|^2.
\tag{11}
$$

To ensure the sparsity of the model, the quadratic error term is replaced, where $h(x_n, w) = W^T X + b$ can obtain a new error function:

$$
\frac{1}{2}\|w\|^2 + C\sum E(h(x_n, w) - y_n).
\tag{12}
$$

Same as the classification model, relaxation factor ξ is introduced, where

$$
\begin{aligned}
y_n &\leq h(x_n, w) + \varepsilon + \xi, \\
y_n &\geq h(x_n, w) - \varepsilon - \xi.
\end{aligned}
\tag{13}
$$

After sorting out, the final error function of the SVM

TABLE 1: Data basis of 3D geological modeling.

| Profile name	Scale	The number of	Detection depth (m)
Topographic geological map	1 : 5000	1	The earth's surface
Geological map of bedrock	1 : 5000	1	The earth's surface
Pillar contrast map of ore bed	1 : 5000	2	1000
Borehole bar diagram	1 : 200	147	70~1030
Geological prospecting section	1 : 2000	21	1000~1200
CSAMT comprehensive interpretation profile	1 : 10000	12	2000
Middle section of CSAMT comprehensive interpretation	1 : 10000	3	500, 1000, 1500
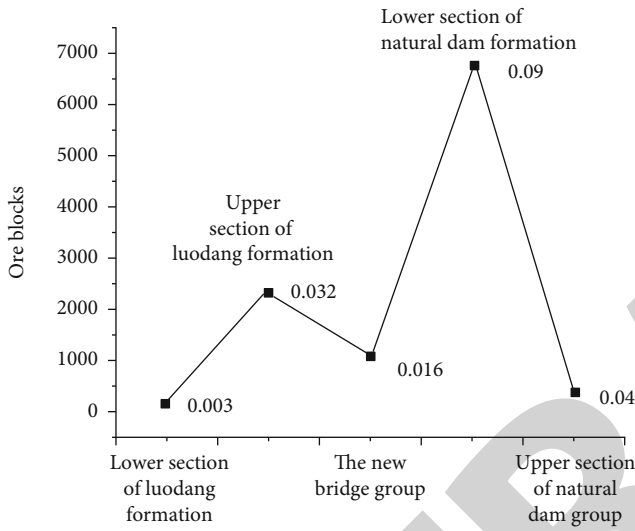
FIGURE 1: Ore-bearing statistics of strata.
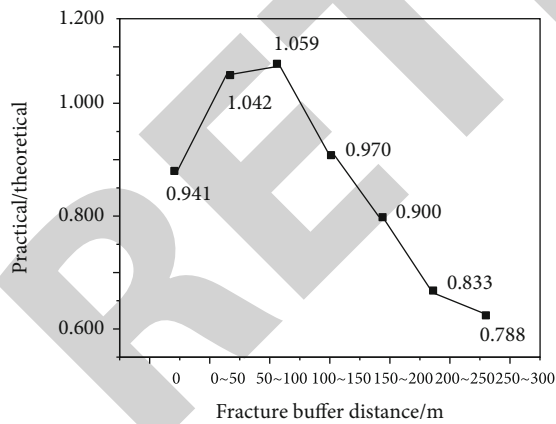
FIGURE 2: Statistics of ore-bearing rate in fracture buffer.

regression model is

$$\frac{1}{2} \|W\|^2 + C \sum \left(\widehat{\xi} + \xi \right). \tag{14}$$

The specific solving process of this model is the same as that of the SVM classification model.

3. Three-Dimensional Geological Modeling

3D geological modeling is an important basis for 3D geological mapping, deep geological survey, and large-scale 3D metallogenic prediction of key metallogenic zones and also an important way to solve some deep geological problems and study geological laws. Surpac6.3, the 3D modeling software of GEMCOM International Mining Software Co., LTD., was adopted for this 3D geological modeling based on plane geological map, borehole data, exploration line profile, and geophysical comprehensive interpretation map. The modeling data are shown in Table 1. Section modeling method was adopted to construct three-dimensional solid models of stratum, rock mass, fault, low resistivity anomaly, and ore body in the study area "vertical cube" [17]. The coordinate range of modeling in this study is 2899615~2903025 m from north to south, 792980~796250 m from east to west, and 1000~2050 m above sea level. Considering the spacing of boreholes, the spacing of geological section exploration lines, the amount of data after subdividing 3D geological solid model blocks, and the computer computing capacity, the running speed of the computer can be improved as much as possible on the premise that the size of block units can meet the calculation accuracy of 3D metallogenic prediction. Therefore, the whole solid model area was divided into blocks according to the block unit size of 25 m × 25 m × 25 m, and the total number of block units divided in the whole research area was 3,099,906. There are a large number of vein ore bodies in the study area. When dividing the whole study area with the above-mentioned unit block size, as long as ore bodies are included, they are assigned as vertical blocks of ore bodies, and there are a total of 14064 known ore bodies. It should be pointed out that it is extremely inaccurate to divide ore bodies at this scale for reserve estimation, but the block model constructed is intended to serve as positive sample markers in a wireless sensor [18, 19].

4. Three-Dimensional Energy Prediction

4.1. Extraction of Favorable Metallogenic Information. In the process of energy prediction, it is the prediction model that finally decides which GIS layer participates in the model operation. The prediction model is based on the prospecting model, through the cube (or grid unit) to establish the characteristic variables of different parts, and combined with the
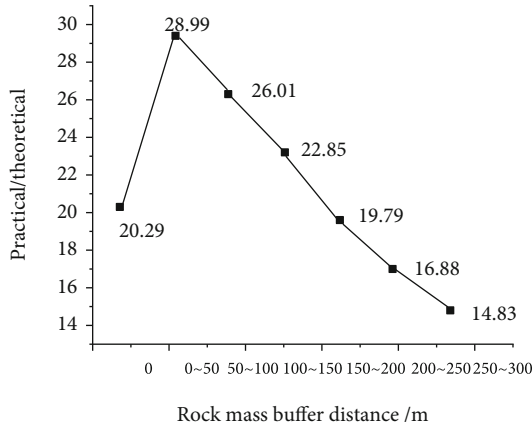
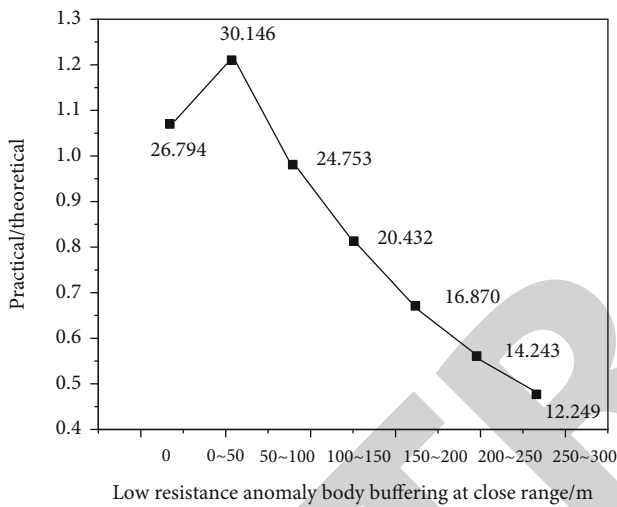Figure 3: Statistics of ore-bearing rate of rock mass buffer.

Figure 4: CSAMT low resistance anomaly buffer ore-bearing rate statistics.

known ore body (or ore point) to analyze and extract the favorable conditions for mineralization, and finally, the ore-controlling elements and their favorable metallogenic range are combined to form the prediction model. In this study, favorable information of mineralization was extracted from stratigraphy, structure, rock mass, and geophysics.

4.2. Formation Favorable Information. Five stratigraphic units are mainly modeled in this study. The number of ore bodies contained in different stratigraphic blocks is shown in Figures 1–4. If we consider the difference of distribution range of different strata, we can use the concept of ore-bearing ratio for comparative analysis. The ore-bearing rate can be obtained by the number of ore bearing in different strata/the number of formation blocks (Figure 1). The ore-bearing rate is the highest in the lower Tiantianba Formation, followed by the upper, Xinqiao, upper and lower Tiantianba Formation of Luodang Formation. Through the statistical analysis of the above two aspects, it can be found that the main ore-bearing strata in the Hongnipo mining area are the lower member of Tiantianba Formation and the upper member of Luodang Formation.

4.3. Construct Favorable Information. The formation of Hongnipo copper deposit is closely related to regional basement faults. From the perspective of extraction of favorable metallogenic information energy, the number of fault blocks in the study area is 41462, and the number of superposition with ore bodies is 110, so the ore-bearing rate of the fault is 0.0025, reaching a certain level of ore-bearing rate. Therefore, the fault is the ore controlling factor for energy prediction. In addition, ore-forming migration channels are often characterized by fault buffer zones. In this paper, the "expansion buffer method" is used to quickly build the fault buffer of different distances and then determine the best fault buffer distance through the analysis of ore bearing. The expansion buffering method adopts the expansion algorithm in morphological analysis and applies it to the 3D block model. The size of the cube model in this study is 25 m, and one square is buffered each time, 25 m distance. The buffer of $0 \sim N * 25$ m can be obtained by N times of buffering, and the model obtained by $n - 1$ times of buffering can be removed to achieve different grades of fracture buffer block model. Statistical results of fracture buffer in this study are shown in Figure 2. When the fracture buffer is 100 m, it is the optimal fracture buffer distance. In addition to the direct analysis of faults and their buffer zones, favorable metallogenic information can often be mined by energy analysis of the characteristic parts of faults in energy prediction.

4.4. Favorable Information of Rock Mass. In this three-dimensional geological modeling of rock mass, only gabbro and gabbro intercalated breccia are constructed, which are collectively referred to as "rock mass" in energy prediction. In the block model, the total number of rock mass is 35812, among which the number of ore-bearing blocks is 584, and the ore-bearing rate is 0.016, reaching a certain level of ore-bearing rate. Therefore, rock mass is the ore-controlling factor for energy prediction. Similarly, through statistical analysis of "expansion buffer method" in this study, when the rock mass buffer range is 50 m, the ratio of actual and theoretical ore concentration in the buffer reaches 28.993, so the rock mass buffer distance is determined to be 50 M (Figure 3).

4.5. Geophysical Favorable Information. The CSAMT method adopted in this study plays an important role in stratigraphic division, fault location, and rock mass inference. In addition, through the superposition analysis of apparent resistivity profile and known ore body, combined with the ore-controlling environment of the study area and the interpretation and inference results of each survey line, 12 middle-low resistivity abnormal areas are delineated on 12 comprehensive interpretation profiles, and then, three-dimensional reconstruction is carried out to form mineralized abnormal bodies. The total number of vertical blocks of abnormal mineralized bodies is 32033, including 1407 ore blocks, and the ore-bearing rate is 0.044. Since the apparent resistivity is continuous and the medium and low resistivity are defined as relative regions, information leakage can be reduced as much as possible by making buffers. The

TABLE 2: Quantitative prediction model of copper mine.

Types of ore deposits	Ore-controlling factors	Element type	Characteristics of the variable	The eigenvalue
Volcanic sedimentary metamorphism Type E copper (iron) ore	Formation	Ore formation	A natural dam group	A natural dam group
			The new bridge group	The new bridge group
			Fall dang group	Fall dang group
	Structure	Ore-controlling fracture	Basement faults	The fracture
		Fracture zone	Rupture zone	The 100 MB buffer
		Tectonic site	Azimuth anomaly	(0, 0.1)
			Structural isodensity	(1.045, 1.492)
			Degree of central symmetry	(0.001, 0.210)
			Structural frequency	(0, 1.375)
	Rock mass	Favorable ore-forming rock	Gabbro	Gabbro
		Rock contact zone	Rock buffer zone	Buffer 50 m
		Favorable rock characteristics	Rock mass differentiation	(0.07, 3.04)
	Geophysical	Abnormal apparent resistivity	CSAMT abnormal	Low resistivity abnormal body
			CSAMT exception buffer	Buffer 50 m

"expansion buffer method" was adopted to analyze the ore-bearing rate under different buffer zones, and the optimal buffer distance was determined to be 50 m (Figure 4). Based on the above extraction of metallogenic information and combined with the regional mineral characteristics of the study area, the three-dimensional energy prediction model of copper mine is formed (Table 2), as shown in Table 2.

4.6. Classification of Ore-Forming Energy. The ore-forming energy anomalies delineated in the study area are classified according to the following principles:

(1) There should be 3 or more geochemical sampling points within the anomaly

(2) For small anomalies with sampling points less than 3, if they belong to the same third-order catchment basin, several small anomaly groups with the same anomaly source can be divided into one anomaly according to the drainage distribution and the relationship between sampling points

(3) The anomaly numbers are individually numbered according to the four geochemical subzones, in the form of "E3-2," where *E* represents the comprehensive anomaly of metallogenic energy, 3 represents geochemical partition, and 2 is the sequence number of the anomaly

5. Conclusions

In this study, a machine learn-based study on geological and mineral energy and mineral energy classification was proposed, and a three-dimensional geological entity model was constructed. After the cube of the entity model, the three-dimensional quantitative prediction model of the study was determined through the extraction of metallogenic information. Under the guidance of the quantitative prediction model, the wireless sensor algorithm was used to carry out the 3D quantitative prediction based on the wireless sensor algorithm. The training accuracy of the model and the test accuracy of the model were over 96%, which proved the accuracy of the RF model construction and achieved satisfactory results. In this study, a wireless sensor is successfully applied to 3D mineral energy prediction, which makes a positive exploration for mineral resource prediction and evaluation in the future. Finally, the prediction of mineral resource energy based on a wireless sensor is an important trend of future development.

Data Availability

The data used to support the findings of this study are available from the corresponding author upon request.

Conflicts of Interest

The authors declare no conflicts of interest.

References

[1] X. Huang, J. Sun, S. M. Srinivasan, and R. S. Sangwan, "Comparative study of disease classification using multiple machine learning models based on landmark and non-landmark gene expression data," *Procedia Computer Science*, vol. 185, no. 1, pp. 264–273, 2021.

[2] Y. Chen, J. Tao, J. Wang et al., "The novel sensor network structure for classification processing based on the wireless sensor method of the acgan," *Sensors*, vol. 19, no. 14, p. 3145, 2019.

[3] C. Frederick, S. Villar, and Z. H. Michalopoulou, "Seabed classification using physics-based modeling and machine learning," *The Journal of the Acoustical Society of America*, vol. 148, no. 2, pp. 859–872, 2020.

[4] P. Rückert, B. Papenberg, and K. Tracht, "Classification of assembly operations using machine learning algorithms based on visual sensor data," *Procedia CIRP*, vol. 97, no. 1, pp. 110–116, 2021.

[5] G. Fu, Q. Lü, J. Yan et al., "3D mineral prospectivity modeling based on machine learning: a case study of the Zhuxi tungsten deposit in northeastern Jiangxi Province, South China," *Ore Geology Reviews*, vol. 131, no. 4, article 104010, 2021.

[6] J. Bhatia, A. Dayal, A. Jha et al., "Classification of targets using statistical features from range fft of mmwave fmcw radars," *Electronics*, vol. 10, no. 16, p. 1965, 2021.

[7] S. Nurmaini, A. Darmawahyuni, A. N. Sakti Mukti, M. N. Rachmatullah, F. Firdaus, and B. Tutuko, "Deep learning-based stacked denoising and autoencoder for ecg heartbeat classification," *Electronics*, vol. 9, no. 1, p. 135, 2020.

[8] C. V. Aravinda and M. Lin, "Wireless sensor-based apathy classification on doppler radar image for the elderly person," *Procedia Computer Science*, vol. 187, no. 3, pp. 146–151, 2021.

[9] N. Siomos, I. Fountoulakis, A. F. Bais, T. Drosoglou, and A. Natsis, "Automated aerosol classification from spectral uv measurements using wireless sensor clustering," *Remote Sensing*, vol. 12, no. 6, p. 965, 2020.

[10] Z. Meng, F. Zhao, M. Liang, and W. Xie, "Deep residual involution network for hyperspectral image classification," *Remote Sensing*, vol. 13, no. 16, p. 3055, 2021.

[11] M. Usman, M. Shamim, Z. Ahmad, M. Zaidi, and S. Jaffar, "Heart rate detection and classification from speech spectral features using wireless sensor," *Archives of Acoustics*, vol. 46, no. 1, pp. 41–53, 2021.

[12] J. Kang, Z. Ullah, and J. Gwak, "Mri-based brain tumor classification using ensemble of deep features and machine learning classifiers," *Sensors*, vol. 21, no. 6, p. 2222, 2021.

[13] H. Arab, I. Ghaffari, L. Chioukh, S. Tatu, and S. Dufour, "Machine learning based object classification and identification scheme using an embedded millimeter-wave radar sensor," *Sensors*, vol. 21, no. 13, p. 4291, 2021.

[14] A. Chatterjee, H. Woodruff, M. Lobbes, Y. V. Wijk, and P. Lambin, "Altering the decision threshold as a simple and effective method for machine learning-based classification of imbalanced radiation oncology data," *International Journal of Radiation Oncology • Biology • Physics*, vol. 108, no. 3, article e332, 2020.

[15] Z. Zhang, Y. Zhang, L. Ying, C. Sun, and H. F. Zhang, "Machine-learning based spectral classification for spectroscopic single-molecule localization microscopy," *Optics Letters*, vol. 44, no. 23, pp. 5864–5867, 2019.

[16] Y. Deng, C. Cao, and S. Chen, "Research on correlation analysis and prediction model of agricultural climate factors based on machine learning," *MATEC Web of Conferences*, vol. 336, no. 7, article 07016, 2021.

[17] W. Jiang, X. Xing, X. Zhang, and M. Mi, "Prediction of combustion activation energy of NaOH/KOH catalyzed straw pyrolytic carbon based on machine learning," *Renewable energy*, vol. 130, pp. 1216–1225, 2019.

[18] M. He, Y. Xu, and N. Li, "Population spatialization in Beijing city based on machine learning and multisource remote sensing data," *Remote Sensing*, vol. 12, no. 12, p. 1910, 2020.

[19] Y. Sun, L. Guan, M. Wu, Y. Gao, and Z. Chang, "Vehicular navigation based on the fusion of 3d-riss and machine learning enhanced visual data in challenging environments," *Electronics*, vol. 9, no. 1, p. 193, 2020.